

Implementation of an X-Band Phased-Array Subsystem in a Deep Space Mission

Dipak K. Srinivasan, Robin M. Vaughan, Robert E. Wallis, M. Annette Mirantes,
T. Adrian Hill, Sheng Cheng, Jonathan R. Bruzzi, and Karl B. Fielhauer
The Johns Hopkins University
Applied Physics Laboratory
11100 Johns Hopkins Road
Laurel, MD 20723
443-778-7107
dipak.srinivasan@jhuapl.edu

Abstract—The MESSENGER spacecraft, the first mission to the planet Mercury since 1975, will achieve Mercury orbit in 2011. The spacecraft uses two opposite-facing mission-enabling X-band (8.4 GHz) phased-array antennas to achieve high-rate downlink communications. The spacecraft orientation is constrained such that a preferred direction faces the Sun; rotation about the Sun-line is allowable. The main beam of each antenna is steerable in one dimension. These two degrees of freedom allow the main beam of the phased array to be pointed in any direction about the spacecraft. A novel system-level design requires many different subsystems of the spacecraft to interact together to achieve accurate beam-pointing, and thus, high-rate downlink data from Mercury to Earth.^{1,2}

Once at the planet, the solar flux intensity will be as large as 11 times that seen on the Earth; this is mitigated by a sunshade made of a heat-resistant ceramic cloth that shields the main body of the spacecraft from the intense +300°C heat. However, proper sunshade operation places an attitude constraint on the spacecraft; the sunshade-normal vector must be within a “Sun Keep-In (SKI) Zone” with respect to the spacecraft-Sun line to prevent direct solar radiation from reaching the spacecraft main body. The SKI Zone requirement prevents the spacecraft from being rotated about any arbitrary axis. However, spacecraft rotation about the spacecraft-Sun line and small deviations within the SKI Zone (up to 12°) are allowable because of the slightly oversized sunshade.

TABLE OF CONTENTS

1. INTRODUCTION	1
2. PHASED ARRAY CONCEPT AND OVERVIEW	1
3. SYSTEM IMPLEMENTATION	3
4. TESTING AND VERIFICATION	8
5. IN-FLIGHT PERFORMANCE	8
6. CONCLUSIONS	9
ACKNOWLEDGEMENTS	9
REFERENCES	10
BIOGRAPHIES	10

1. INTRODUCTION

The MErcury, Surface, Space ENvironment, GEOchemistry, and Ranging (MESSENGER) spacecraft, the first mission to orbit the planet Mercury, was launched on 3 August 2004 from Cape Canaveral Air Force Base [1]. The seven-year cruise includes one Earth flyby, two Venus flybys, and three Mercury flybys before Mercury Orbit Insertion. With an inner-planet trajectory, the Earth can be in any direction about the spacecraft. The need for a high-gain downlink in all directions poses a significant system design challenge. MESSENGER is a Discovery Program mission designed, built, and managed by The Johns Hopkins University Applied Physics Laboratory (APL).

A traditional parabolic high-gain antenna was not an option for MESSENGER. Because of the SKI Zone constraint, any high-gain dish would have to be a gimbaled dish to achieve antenna-pointing. A fixed dish would require the entire spacecraft to be rotated. The harsh thermal environment would cause distortions in the antenna pattern of a traditional parabolic dish. Furthermore, two gimbaled dishes (necessary because of the inner-planet trajectory and spacecraft pointing requirements) would exceed spacecraft packaging constraints. The solution was to implement two electronically steerable phased arrays on the spacecraft. Each phased array can scan $\pm 60^\circ$ in one dimension, with the other dimension provided by the roll about the spacecraft-Sun line. These characteristics allow a high-gain downlink to be achievable in all directions about the spacecraft [2].

2. PHASED ARRAY CONCEPT AND OVERVIEW

The MESSENGER spacecraft has two diametrically opposite-facing phased-array antennas for high-gain downlink communications as shown in Figure 1. Each array is capable of one-dimensional scanning $\pm 60^\circ$ about its boresight in the XY plane of Figure 1. The combination of

¹ 0-7803-8870-4/05/\$20.00© 2005 IEEE

² IEEEAC paper #1067, 10 December 2004

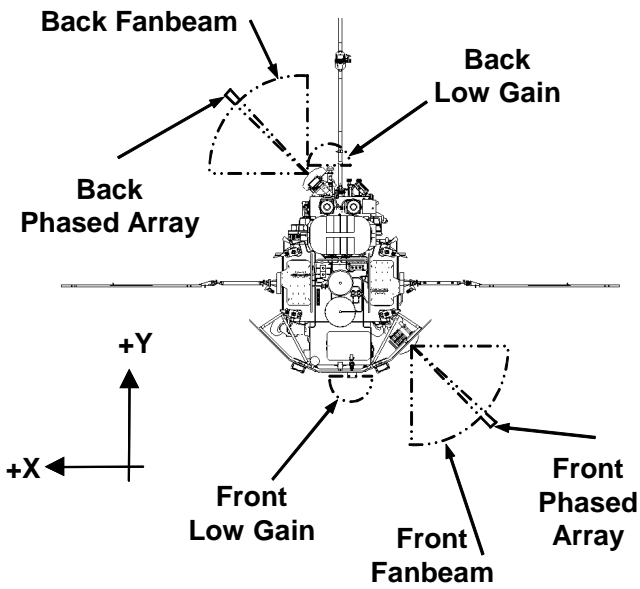


Figure 1. MESSENGER Antenna Coverage

this scanning and spacecraft rotation about the Sun-axis allows the main antenna beam to be pointed in any direction. Nominally, each array will be used to $\pm 45^\circ$ about its boresight, with the spacecraft rotation allowing communication in the other two quadrants. However, the added 15° of operation allows greater flexibility in the operations of the spacecraft if rotation and/or switching to the other phased array need to occur at an undesirable time.

The Guidance and Control (G&C) Subsystem must orient the spacecraft such that the Earth line is in the scanning plane of the phased arrays while placing the Sun line at the desired offset from the shade normal (spacecraft $-Y$ axis) within the constraint zone. The nominal downlink attitude aligns the $-Y$ axis with the Sun line, but offsets between these directions may be used for passive momentum control using sunshade solar torque. The G&C subsystem continuously computes the directions to the Earth and Sun using on-board time and ephemeris models. It evaluates the Sun-probe-Earth (SPE) angle to determine which of the opposing phased arrays to use and the angle to which the array must scan.

The scan angle for the array is used to determine which entry in a programmable look-up table should be used for the exact phase settings necessary to steer the antenna beam to the Earth. The flight software must take into account current spacecraft conditions and modify the phase settings depending on which transponder is being used (see Figure 2). This modification compensates for the 90° phase lag introduced by the cross-path of the Hybrid Coupler when the transponder B exciter is used. This extra mathematical step allows the spacecraft to maintain only two look-up tables (one for each phased array) as opposed to four (one for each transponder-phased array combination). The flight software also has the capability of overriding the G&C control of the phase settings, allowing ground controllers to specify either a different index in the look-up table or a custom phase setting. This capability supports such activities as debugging and commissioning.

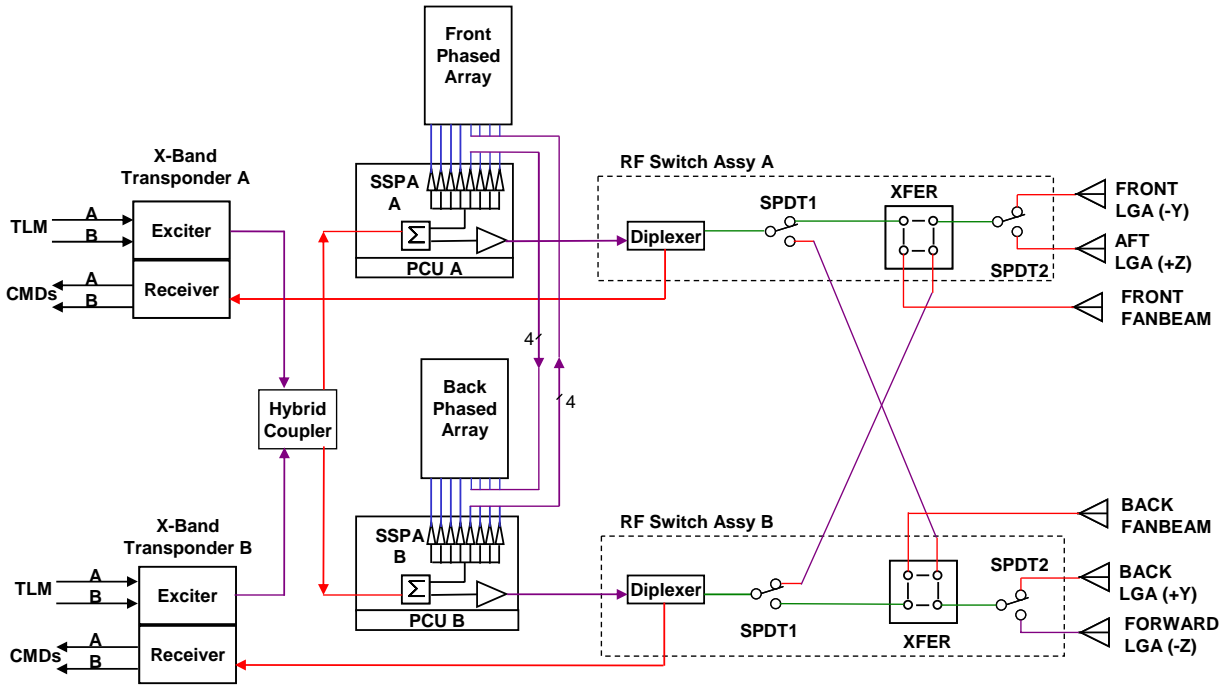


Figure 2. RF Block Diagram.

The phase settings are sent via a 1553 command bus to a Solid-State Power Amplifier (SSPA), which controls the phase of each element. The two SSPAs each have eight distributed “stick” amplifiers consisting of a 4-bit phase shifter (22.5° least-significant-bit [LSB]) and an amplifier chain. The SSPA then feeds the RF signals to the phased-array antenna. Each phased-array antenna is composed of eight radiating elements, each fed by a separate stick of the distributed SSPA. Each element of the phased-array antenna is a slotted waveguide standing wave antenna with attached parasitic elements providing right-hand circular polarization.

The SSPAs and phased arrays are two parts of the overall RF subsystem as shown in Figure 2. Two X-band small deep space transponders, built by General Dynamics, are responsible for receiving and demodulating the RF uplink signal and generating and modulating the RF downlink signal. Only one transponder exciter is on at any given time. The Hybrid Coupler distributes the RF signal to both SSPAs. Each SSPA can be in one of four modes: “Distributed Front,” “Distributed Back,” “Lumped,” and off. The distributed modes provide the RF signals necessary for four of the phased array’s elements, and the lumped mode provides an RF signal to the fanbeam and low-gain antennas.

3. SYSTEM IMPLEMENTATION

Guidance and Control

The G&C software continuously computes the directions to the Sun and Earth using on-board time and ephemeris models. These directions are transformed from the EME2000 inertial frame into the spacecraft body axes, shown in Figure 3, using the current estimated attitude. They are then manipulated as unit vectors or as an azimuth and an elevation angle to obtain other geometric quantities of interest for RF communication. Referring to Figure 3, the azimuth angle, denoted A , is the angle in the XY plane measured clockwise from the $-Y$ axis to the projection of the unit vector in the XY plane. The elevation angle, denoted E , is the angle between the unit vector and the XY plane of the body frame. Elevation is considered to be positive for vectors on the $-Z$ side of the XY plane and negative for vectors on the $+Z$ side of the plane. Thus a unit vector \hat{u} in the body frame can be expressed as $\hat{u} = [u_x \ u_y \ u_z]^T = [\cos E \sin A \ -\cos E \cos A \ -\sin E]^T$ where $-180^\circ \leq A \leq +180^\circ$ and $-90^\circ \leq E \leq +90^\circ$. Let \hat{e} be the unit vector to the Earth and A_e and E_e be the Earth azimuth and elevation angles.

The G&C software uses A_e to determine the look-up table and index in that table that are needed to steer the phased-array antennas. The azimuth limits defining the boundaries of each antenna’s scan range in the XY plane are parameters that are specified to the software. The boresights for the front and back antennas are at azimuth angles of -45° and 135° , respectively. Given the 60° scan range in both directions from this boresight, the look-up table boundaries

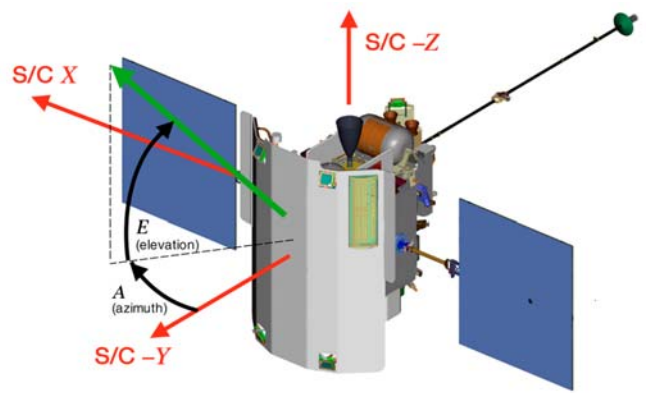


Figure 3. Spacecraft Coordinate System

are set to -105° and 15° for the front antenna and to 75° and -165° for the back antenna as shown in Figure 4. The front table is selected when $-105^\circ \leq A_e \leq +15^\circ$ and the back table when $75^\circ \leq A_e \leq 180^\circ$ or $-180^\circ \leq A_e \leq -165^\circ$. The look-up table for each antenna contains 121 entries for scan or azimuth angles in 1-degree increments over the 120-degree scan range. The index is set to that of the closest scan angle when A_e is within one of the scan ranges. It is set to the edge of the nearest region when A_e is outside both antenna scan ranges (index = 0 or 120).³ These two phased array steering parameters are passed to the phased-array controller task at a 1-Hz rate, regardless of the actual spacecraft attitude. For successful phased-array communications, E_e must be near zero ($<1.5^\circ$ in magnitude) and A_e must be in one of the antenna scan ranges. Ensuring proper values of A_e and E_e requires manipulating the spacecraft attitude as described below.

The G&C subsystem provides a special pointing command to place the spacecraft in a downlink attitude. This attitude

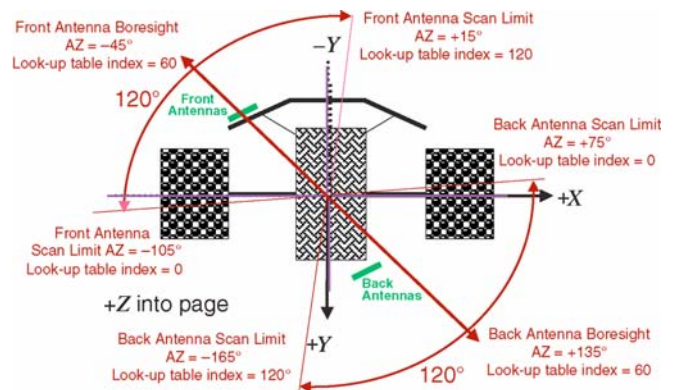


Figure 4. Phased Array Scanning Coverage

³ In the unlikely event that on-board time or ephemeris knowledge is lost, the software sets the table and index assuming that the Earth is aligned with the $-Y$ axis. This is the nominal attitude of the spacecraft.

simultaneously puts the Sun in a desired direction in the body frame and the direction to Earth in the scan range of one of the phased-array antennas. For most of the mission, the Sun direction defaults to the $-Y$ axis so that the sunshade faces the Sun. When specifying spacecraft attitude, a separate set of limits—inside the actual scan range—is used to define a “field of view” for each antenna. Nominally, the antennas are assumed to cover only a 90° quadrant of the XY plane instead of the full 120° scan range as shown in Figure 4. The angular limits defining the boundaries of each antenna’s field of view and the axis to be aligned with the Sun are parameters that are specified to the software when the downlink attitude is selected. The choice of which quadrant, and hence which antenna, to use is dictated by the separation angle between the vectors to the Earth and the Sun as seen from the spacecraft, denoted θ_{es} . When $\theta_{es} < 90^\circ$ and the $-Y$ axis points to the Sun, the Earth vector must lie in the $-X, -Y$ quadrant so that the antenna mounted on the sunshade is used. When $\theta_{es} > 90^\circ$ and the $-Y$ axis points to the Sun, the Earth vector must lie in the $+X, +Y$ quadrant, and the antenna mounted on the back side of the spacecraft structure is used. The opposite choices for antenna apply when the $+Y$ axis points to the Sun: the back antenna is used when $\theta_{es} < 90^\circ$ and the front antenna is used when $\theta_{es} > 90^\circ$. The transformation Q_{J2}^D from the inertial frame to the body frame for downlink attitude can be expressed as

$$Q_{J2}^D = \begin{bmatrix} \hat{i}_x^T \\ \hat{i}_y^T \\ \hat{i}_z^T \end{bmatrix} \quad (1)$$

$$\begin{cases} \hat{i}_y = -\hat{i}_s & \text{for } -Y \text{ to Sun} \\ \hat{i}_y = +\hat{i}_s & \text{for } +Y \text{ to Sun} \\ \hat{i}_z = (\hat{i}_e \times \hat{i}_s) / \|(\hat{i}_e \times \hat{i}_s)\| & \text{for } \theta_{es} < 90^\circ \\ \hat{i}_z = (\hat{i}_s \times \hat{i}_e) / \|(\hat{i}_s \times \hat{i}_e)\| & \text{for } \theta_{es} > 90^\circ \\ \hat{i}_x = (\hat{i}_y \times \hat{i}_z) / \|(\hat{i}_y \times \hat{i}_z)\| \end{cases}, \quad (2)$$

where \hat{i}_e and \hat{i}_s are unit vectors from spacecraft to Earth and the Sun in the EME2000 inertial reference frame.

As previously mentioned, SKI Zone constraints allow a small range of offsets of the spacecraft-Sun line from the $+Y$ or $-Y$ axis. This will be exploited to manage the spacecraft momentum through the action of solar torque. The downlink pointing command includes provisions to instruct the software to automatically determine a spacecraft-Sun line offset from the $+Y$ or $-Y$ axis that can achieve a desired target momentum while maintaining the spacecraft-Earth line in one of the antenna fields of view. Let \hat{s} be the desired unit vector to the Sun and A_s and E_s be the Sun

azimuth and elevation angles. To find the attitude offset from the default attitude with $+Y$ or $-Y$ aligned with the Sun that maintains the Earth direction in a region of the XY plane for downlink, first perform a rotation that puts the Sun in this direction. This rotation Q_D^1 is expressed by the XZ Euler rotation sequence

$$Q_D^1 = Q_z(-A_s) Q_x(-E_s), \quad (3)$$

where Q_z is a rotation about the Z axis by the azimuth angle and Q_x is a rotation about the X axis by the elevation angle. The direction to Earth in this intermediate frame is given by $\hat{e}_1 = Q_D^1 Q_{J2}^D \hat{i}_e$.

Next, perform a rotation about the Sun line from this intermediate attitude such that the Earth line moves back into the XY plane. Since the Sun direction is constant under this final rotation, the possible final locations for the Earth vector can be found using the spherical triangle shown in Figure 5. From the law of cosines,

$$\cos \delta = \cos \theta_{es} / \cos E_s. \quad (4)$$

After this final rotation, the unit vector to Earth in the body frame will be $\hat{e}_2 = [\sin(A_s \pm \delta) \quad -\cos(A_s \pm \delta) \quad 0]^T$.

The rotation angle about the Sun line is the angle between the plane containing the vectors to the Sun and the Earth in the intermediate frame and the plane containing the vectors to the Sun and the Earth in the XY plane, \hat{e}_2 . This angle, denoted β , is found using the normals to these two planes as shown below

$$\beta = \cos^{-1}(\hat{\eta}_1 \cdot \hat{\eta}_2), \quad (5)$$

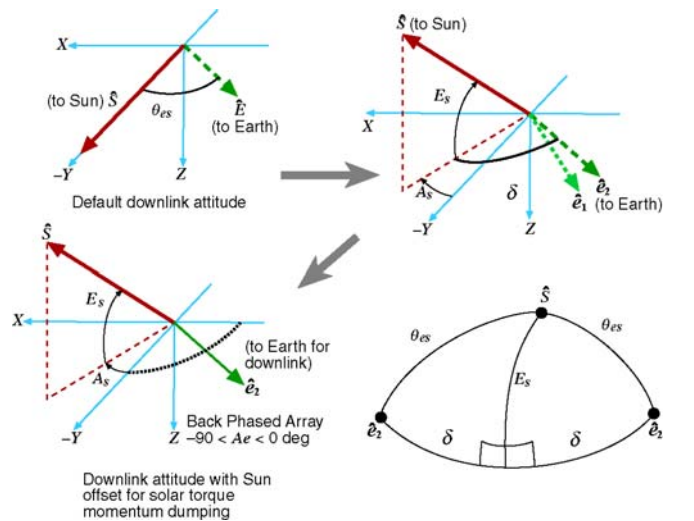


Figure 5. Spacecraft Rotations for Downlink Attitude

where

$$\begin{aligned}\hat{\eta}_1 &= (\hat{s} \times \hat{e}_1) / \|\hat{s} \times \hat{e}_1\| \\ \hat{\eta}_2 &= (\hat{s} \times \hat{e}_2) / \|\hat{s} \times \hat{e}_2\|\end{aligned}\quad (6)$$

The sign of β depends on which side of the \hat{s}, \hat{e}_2 plane contains the \hat{e}_1 vector:

$$\begin{aligned}\beta &> 0 \text{ if } \eta_2 \cdot \hat{e}_1 > 0 \\ \beta &< 0 \text{ if } \eta_2 \cdot \hat{e}_1 < 0\end{aligned}\quad (7)$$

Let Q_1^2 be the rotation matrix representing the rotation about \hat{s} by angle β ; then the rotation from the inertial frame to the desired offset downlink attitude is

$$Q_{J2}^2 = Q_1^2 Q_D^1 Q_{J2}^D. \quad (8)$$

When the desired \hat{s} lies outside the SKI Zone, A_s and E_s are changed to place the Sun's direction on the boundary of the zone as close as possible to \hat{s} . The Earth-Sun geometry places another restriction on E_s . Solutions to Eq. (3) for δ only exist when $E_s \leq \theta_{es}$. This supercedes the SKI Zone limitation in cases where θ_{es} is smaller than the SKI Zone elevation boundary in magnitude. Finally, A_e must fall in one of the phased-array antenna fields of view. In general, there are two solutions for δ and hence for β ; the choice of which to use is made based on the resulting value of A_e . In rare cases, neither choice will satisfy the quadrant restrictions on A_e , and it is necessary to adjust A_s and E_s until A_e moves back into one of the phased-array antenna quadrants. All these constraints mean that the target value for system momentum components may not be met, but the solar torque will act to move the momentum components as close as possible to the target values while still satisfying the constraints on A_s , E_s , and A_e [3].

PAC Table Creation

The phased-array controller (PAC) look-up tables (one for each phased array) correlating scan direction and the state of each of the 4-bit phase-shifters were created on the ground and stored in spacecraft memory, although table updates are possible. Two simple phase measurements were performed to properly calibrate the phased-array antennas. One was performed prior to spacecraft integration to determine the relative radiated phases of the antenna elements (radiated phase offset vector, ϕ_{rad}). The other was performed during spacecraft integration to determine the differences in phase path to the feed of each antenna element (coax phase offset vector, ϕ_{coax}). These two measurements were the only external inputs required to create properly calibrated scan look-up tables for each of the two phased arrays. The phasing increment (Δ) in degrees for each electrical scan angle was determined through

$$\Delta = 180^\circ \times \sin \Theta, \quad (9)$$

where Θ is the desired beam-steer angle off antenna boresight and the electrical length between array-elements is 180° . The required phase state (0 to 15) for each 4-bit phase-shifter (22.5° LSB) was determined through

$$M = \text{mod}\left(\frac{(N-1) \times \Delta - \phi_{coax} - \phi_{rad}}{22.5^\circ}, 16\right), \quad (10)$$

where M is an integer between 0 and 15 representing phase-shifter state and N is an integer between 1 and 8 representing antenna stick element position. The individual phase states of each stick expressed as 4-bit binary words were then combined in groups of four elements and stored in spacecraft memory as two hexadecimal words constituting the PAC look-up table.

Flight Software

The Command and Data Handling (C&DH) flight software runs a Phased-Array Controller task at 1 Hz. This task is primarily responsible for sending the appropriate phase settings to the SSPAs via MIL-STD-1553B bus. It also reads an echo of the phase settings from the SSPAs via the 1553 bus and provides these readings in telemetry.

The C&DH flight software maintains two on-board tables; each contains 32-bit phase settings for every angle between -60° and $+60^\circ$ in 1-degree increments (121 entries spanning a 120° field of view). One table supports the front phased-array antenna while the second supports the back phased-array antenna. Both tables have values that are valid for transponder A. An inversion of 4 of the bits in the 32-bit phase setting is required when transponder B is active, and the C&DH flight software performs this inversion automatically.

There are two modes of software control for the phased arrays. The default and nominal mode places the phase settings under the control of the G&C subsystem. Under G&C control, the C&DH receives the phased-array antenna table (front or back) and index into the table (0 ... 120) from the G&C subsystem software. The C&DH flight software performs a table look-up to extract the proper 32-bit pattern performing bit inversion for transponder-B if necessary. The resulting phase setting pattern is sent to both SSPAs via the 1553 bus. This process is repeated every second with the G&C subsystem re-computing the appropriate table and index to steer the array as shown in Figure 6.

The second mode of software control is bypass mode. In this mode, the C&DH flight software ignores the G&C inputs and follows a user-specified commanded input. Two bypass options are available. The first bypass command allows the user to specify the table and index; the C&DH flight software will perform the same type of table look-up

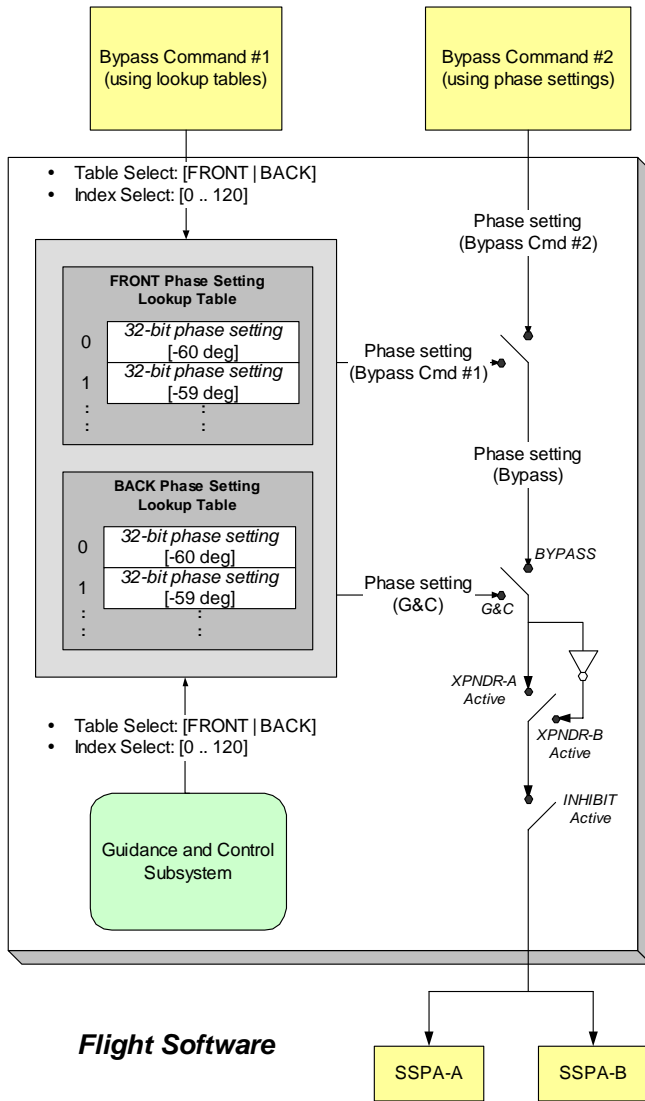


Figure 6. Flight Software Block Diagram

as when under G&C control to produce a 32-bit phase setting; this is useful for deliberate off-pointing of the phased array, which is done during commissioning activities. A second bypass command circumvents the tables entirely and allows the user to specify the 32-bit phase setting directly; this is useful for debugging purposes. In either case, the C&DH flight software still automatically performs the bit inversions to the phase setting if transponder B is active. Unlike the G&C control mode, where the phase settings are sent once per second, in bypass mode the phase setting pattern is only written once (to both SSPAs) per command invocation.

The C&DH flight software can also be commanded to inhibit phase setting commands from being issued to the SSPAs for up to one hour. This provides a mechanism to freeze the phase settings without updates if that is desired.

The two phase setting look-up tables are stored in both volatile RAM and in nonvolatile EEPROM on board the

spacecraft. The RAM version represents the tables actively in use by the C&DH flight software while the EEPROM version is used to initialize the RAM versions after a flight processor reset. Both the RAM and EEPROM versions of the table can be reloaded in flight.

Solid-State Power Amplifier and Phased-Array Controller

There are two SSPAs on board the MESSENGER spacecraft. The RF input signal in the SSPA is equally divided eight ways. Each of the eight-way divider output feeds one of the eight identical phase shifter/amplifier chains referred to as stick amplifiers. Each stick amplifier consists of a 4-bit phase shifter (22.5° increments), a small signal amplifier, a driver amplifier, a power amplifier, and an isolator as shown in Figure 7. The total gain of the stick amplifier is approximately 30 dB from the input of the phase shifter to the output of the isolator. To suppress the possible cavity feedback oscillation of the stick amplifier, waveguide-like structures were built around each stick; microwave absorbers were also added to suppress any high-frequency oscillation. The output power of each stick amplifier is approximately 34 dBm. The SSPA also has a separate 40-dBm output side called lumped amplifier for the low-gain and fan-beam antenna.

Because of thermal constraints, only four of the eight stick amplifiers can be turned on at the same time. This keeps the channel temperature of the amplifier final stages sufficiently low (+125°C) to ensure that the median time to failure is approximately 4×10^6 hours, greatly exceeding the mission requirement. DC power distribution relays inside the SSPA, which are controlled by the PDUs (Power Distribution Units) on board the spacecraft, determine which group of amplifiers is turned on. The SSPA DC power sequencing and PDU command interlocks prevent hot-switching the groups of amplifiers in the SSPA.

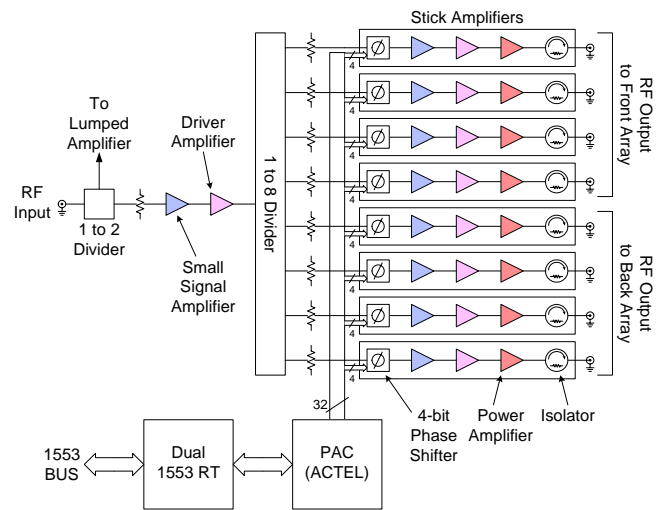


Figure 7. SSPA Block Diagram

The 4-bit phase shifter state in each stick amplifier is controlled by the Phased-Array Controller (PAC) which is implemented by an Actel FPGA on the digital board in the SSPA. A 32-bit register in the Actel provides the phase bit signals to the eight stick amplifiers. These phase bits in the Actel register can be set and read by the spacecraft processor via the 1553 bus. A dual 1553 Remote Terminal hybrid on the SSPA digital board provides the communication link between the SSPA and the spacecraft processor.

Phased-Array Antenna

The phased array is composed of eight waveguide “sticks,” each with 26 slotted radiating elements, and is shown in Figure 8. Each waveguide stick is a standing wave array using narrow wall slots. The use of WR-90 aluminum waveguide with 0.051-cm (0.020-inch) thick walls keeps the mass of each waveguide stick to less than 100 g. The waveguides are fed from the center via an H plane tee. Although the standing wave array design is inherently narrowband, the center-fed approach results in a factor-of-two improvement in the impedance bandwidth compared with an end-fed approach and provides a measured 1-dB antenna gain bandwidth of 1.6%.

Waveguide arrays with slots in the narrow walls are inherently linearly polarized and have traditionally required additional single or multiple layer structures to achieve circular polarization. A combination of parasitic monopoles attached next to the radiating slots and a single dummy waveguide mounted to either side of the eight radiating sticks produces right-hand circular polarization and enables operation over the array’s extreme environment of -150° to $+315^{\circ}\text{C}$. The technology required to enable the high-temperature operation and the electromagnetic principles behind this novel approach to produce circular polarization are described elsewhere [4].



Figure 8. Phased-Array Antenna. It measures 11 inches by 32 inches.

The array 3-dB beam widths are roughly 2° in the narrow plane and 12° in the broad plane. The array is scanned in the plane of the broad beam to minimize the number of cables and phase-shifter modules compared with narrow beam scanning. In addition, broad beam scanning results in less pointing loss caused by phase errors.

Because of the extreme operating temperature range and relatively narrow antenna bandwidth, the gain response of the antenna at the downlink frequency can vary significantly as a function of temperature. To minimize this variation, each antenna stick is tuned by a fine adjustment in the short circuit position at each end of the stick to optimize the gain response with respect to frequency and, equivalently, the temperature. Once the short circuit position adjustment is completed, the short circuits are secured in place with mounting screws. This short circuit also provides the interface for a loop coupler that is temporarily installed to support phased-array systems performance testing at the spacecraft level [3]. Figure 9 shows the measured gain response versus frequency and temperature for the phased array. This response was tuned to favor the higher temperatures expected during the orbit phase of the mission when the greatest science return is desired.

The phased-array radomes use space blanket materials that block light, withstand high temperatures, and have low dielectric constants and low dielectric losses. The radome is a three-layer design of 0.025-cm (0.01-inch) thick 3M™ Nextel™ blanket layers separated by 0.953-cm (0.375-inch) thick Q-felt material. Because the Nextel™ layers are thin and the Q-felt dielectric constant is low, the thickness of the Q-felt is not critical to RF performance. The chosen thickness is a compromise between low mass and light-blocking properties. The measured loss of the radome material is less than 0.1 dB over $\pm 60^{\circ}$ scan angles. Figure 10 shows the gain performance of both the front and back phased arrays.

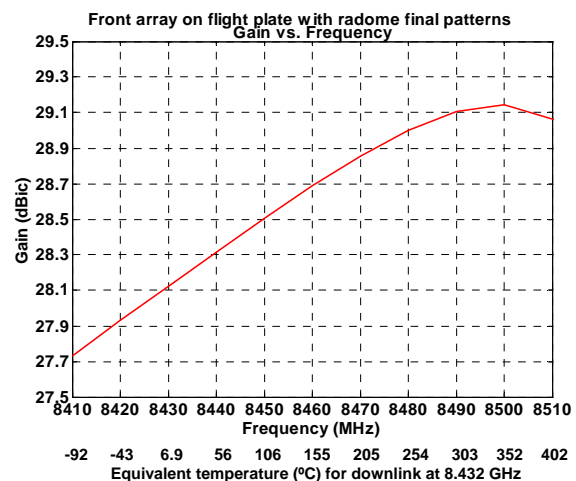


Figure 9. Antenna Frequency and Temperature Response

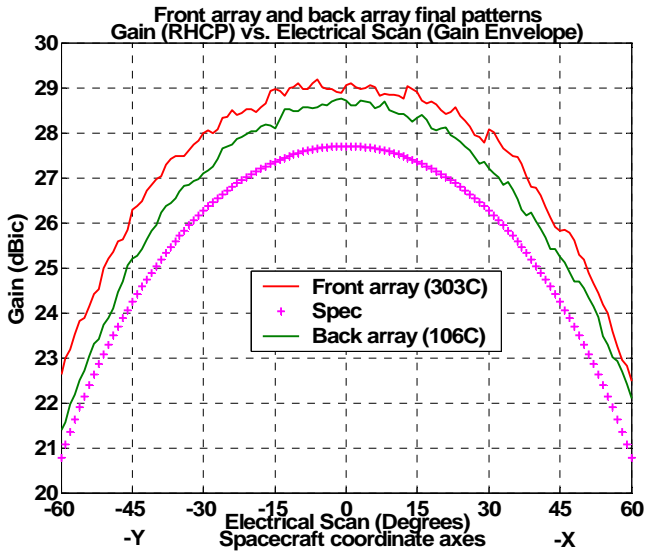


Figure 10. Front and back array gain envelopes at the expected temperatures during Mercury orbit for each array.

4. TESTING AND VERIFICATION

End-to-end tests of the phased-array antenna steering interfaces were performed twice prior to MESSENGER’s launch, once in November 2003 and again in March 2004. The test contained two segments, one where the G&C interface was bypassed to manually command the antenna steering and one where the G&C software provided the antenna steering information. The manual test used software commands to point each antenna along its boresight and to angles offset from the boresight in each direction. These three positions were tested by directly setting the phase shift bit pattern and also by specifying the look-up table (PAC) index. The segment exercising the G&C interface was more comprehensive, testing all entries in each look-up table. A closed-loop dynamic simulation was designed to provide the necessary relative geometry between the spacecraft, the Earth, and the Sun as described below. For both segments, ground support equipment (GSE) was used to capture the signal radiated by each of the phased-array antennas and to analyze it to determine the actual steering direction. This was compared with the commanded steering parameters and the steering direction reported in spacecraft telemetry. Each test segment was executed with transponder A active and then repeated with transponder B active.

The G&C segment of the phased-array steering test first placed the spacecraft in an attitude that had the spacecraft-to-Earth and Sun directions in the XY plane of the spacecraft body frame. Then a series of rotations about the Z axis were executed. Rotating about $+Z$ or $-Z$ caused the Earth vector to rotate in the XY plane so that it moved through each antenna’s scan range. The rotation rate was selected to hold the computed steering direction fixed at each of the 121 indices in the antenna look-up table long enough to measure the actual direction using the RF GSE. The rotations about

the Z axis were repeated as needed to test each combination of phased-array antenna and transponder.

This test method caused the Sun to apparently rotate around the entire body of the spacecraft during the test, so SKI Zone constraints were disabled. Telemetered values for Earth azimuth and elevation angles, selected antenna look-up table, and index in that table were analyzed to confirm proper operation of the G&C flight software.

The actual direction of the phased-array antenna beam was determined by the RF GSE. The RF GSE operated by sampling the phase of the RF signal within each waveguide stick of the phased array using a vector network analyzer as shown in Figure 11. This phased measurement was mathematically summed together to reconstruct the far-field radiated pattern, described as

$$A(\theta) = \sum_{N=1}^{4,8} E_N(\theta) \cdot e^{j\phi_N}, \quad (11)$$

where $A(\theta)$ is the sum pattern, $E_N(\theta)$ is the previously measured element pattern of each individual waveguide stick, and ϕ_N is the measured phase of each element. The summation goes to either 4 or 8, depending on whether the measurement is of a half-array (4 elements illuminated) or full-array (8 elements illuminated).

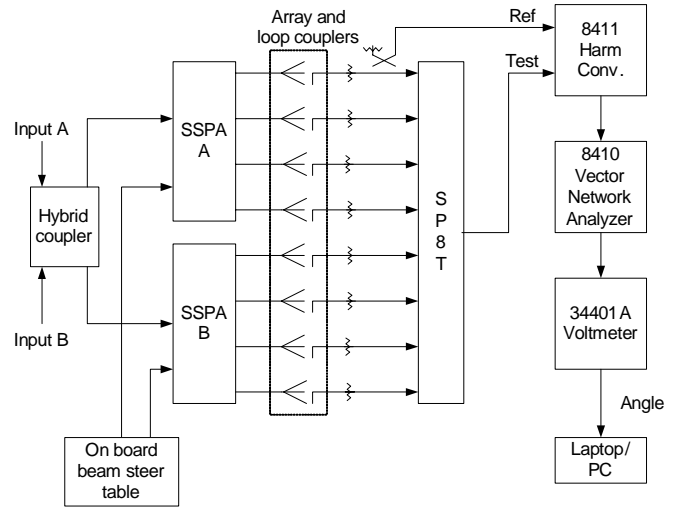


Figure 11. GSE Block Diagram

The reconstructed antenna pattern was plotted by the GSE software in real time to verify proper pointing of the antenna beam [5].

5. IN-FLIGHT PERFORMANCE

After the 3 August 2004 launch, the MESSENGER program began commissioning various subsystems to assess the health of the spacecraft. The first subsystem for checkout

and commissioning was the RF telecommunications subsystem. This was to determine if the spacecraft was in danger of loss of vital command and telemetry; after the checkout was complete, it determined that the RF telecommunications subsystem was in perfect health.

Because of the close proximity to Earth after launch, the commissioning of the phased-array portion of the RF subsystem was postponed for 30 days. The 30-day delay allowed sufficient Earth-spacecraft separation to be achieved to allow accurate commissioning results with the use of a high-gain spacecraft antenna. Deep Space Network (DSN) ground station receivers can become oversaturated and provide false data and performance during early operations if the signal level is too strong [6]. Because of the spacecraft geometry after launch it was not possible to commission the front phased-array antenna system; this will be postponed until about 15 March 2005. Therefore, commissioning consisted only of the back phased-array antenna system.

The objectives of the phased-array antenna commissioning were to determine the following: (1) the peak and scanned gain of the antenna with 4 and 8 antenna elements using both of the spacecraft SSPAs, (2) the proper scan angle and scan direction with both spacecraft transponders, and (3) the state of the pre-programmed PAC table in the spacecraft computer.

To meet the above objectives, it was not feasible nor desirable to rotate the spacecraft position about the spacecraft Z axis. However, it was possible to deliberately off-point the antenna beam from the nominal downlink position based on the SPE angle by putting the phased-array system into bypass mode and asserting specific PAC index settings by ground command. This technique measures the roll-off of the off-pointed antenna, not actual boresight gains as shown in Figure 10. Thus a one-to-one comparison with pre-flight data cannot be accomplished during the commissioning except for the single point. Based on a pre-determined link budget, the degree to which the main antenna beam could be off-pointed was determined with the goal of not losing telemetry and carrier lock of the DSN ground station receivers. Thus, two sets of boundary scan angles were determined for the commissioning based on using 4 or 8 phased-array antenna elements. As the spacecraft geometry over the mission changes, these angles will be expanding to complete the total scan of the antenna.

The results of the back phased-array antenna commissioning are shown in Figure 12. The antenna was scanned 15° off boresight (PAC index of 45) to be in the direction of Earth based on a SPE angle of 60°, and then off-pointed from that scan direction. The values predicted for downlink received power matched the values reported by the DSN Block V Receiver (BVR). Since initial commissioning 30 days post-launch, the back phased array has successfully been used as the primary downlink for the MESSENGER spacecraft.

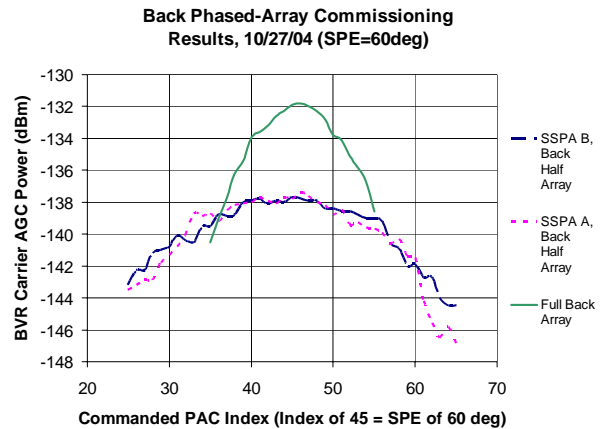


Figure 12. Back Phased-Array Commissioning Results

6. CONCLUSIONS

An innovative system-level design has allowed the MESSENGER mission to sustain a high-rate downlink to Earth by using a novel electronically steered phased-array antenna. The development of this phased-array system required successful interaction between the G&C, flight software, and radio-frequency subsystems. In-flight performance has proven that the system design was sound, as the MESSENGER spacecraft has continued to reliably use the phased-array subsystem for its primary means for downlinking telemetry and data.

ACKNOWLEDGEMENTS

The MESSENGER project is sponsored by the NASA Science Mission Directorate as part of its Discovery Program. The authors wish to thank the large group of individuals who made this effort possible, including Bob Bokulic, Lloyd Ellis, Lee Edwards, Jeff Will, John Penn, Bob Stilwell, James Leary, Bob Nelson, Dave Grosh, and Dave Grant.

REFERENCES

- [1] Andrew G. Santo et al., "The MESSENGER Mission to Mercury: Spacecraft and Mission Design," *Planetary and Space Science*, vol. 49, pp. 1481-1500, 2001.
- [2] Robert S. Bokulic, Karl B. Fielhauer, Robert E. Wallis, Sheng Cheng, M. Lee Edwards, Robert K. Stilwell, John E. Penn, Jonathan R. Bruzzi, and Perry M. Malouf, "MESSENGER Mission: First Electronically Steered Antenna for Deep Space Communications," *Proceedings of the 2004 IEEE Aerospace Conference*, Big Sky, MT, USA, March 2004.
- [3] Robin M. Vaughan, David R. Haley, Daniel J. O'Shaughnessy, and Hongxing S. Shapiro, "Momentum Management for the MESSENGER Mission," paper AAS-01-380, *AAS/AIAA Astrodynamics Specialist Conference*, Quebec City, Quebec, Canada, 30 July – 2 August, 2001.
- [4] Robert K. Stilwell, Robert E. Wallis, and M. Lee Edwards, "A Circularly Polarized, Electrically Scanned Slotted Waveguide Array Suitable for High Temperature Environments," *IEEE Antennas and Propagation Society International Symposium Proceedings*, vol. 3, pp. 1030-1033, 22-27 June 2003.
- [5] Dipak K. Srinivasan, Robert E. Wallis, Jonathan R. Bruzzi, Darryl W. Royster, and Karl B. Fielhauer, "Spacecraft-level Testing and Verification of an X-Band Phased Array," *Proceedings of the 2005 IEEE Aerospace Conference*, Big Sky, MT, USA, March 2005.
- [6] Peter W. Kinman and Jeff B. Berner, "Two-Way Ranging during Early Mission Phase," *Proceedings of the 2003 IEEE Aerospace Conference*, Big Sky, MT, USA, 8-15 March 2003.

BIOGRAPHIES

Dipak K. Srinivasan is a member of the Associate Professional Staff in the RF Engineering Group of the APL Space Department. He received his B.S. in electrical engineering in 1999 and M.Eng. in electrical engineering in 2000 from Cornell University, and an M.S. in applied physics from The Johns Hopkins University in 2003. Mr. Srinivasan joined the APL Space Department in 2000, where he was the lead RF Integration and Test Engineer for the CONTOUR and MESSENGER spacecraft, and is currently the lead RF telecomm analyst for the MESSENGER project.



Robin M. Vaughan is a section supervisor in the Guidance and Control and Mission Analysis Group of the APL Space Department. She has been the MESSENGER guidance and control lead engineer since joining APL in 2000. Prior to joining APL, she worked on interplanetary navigation for the Voyager 2, Galileo, Cassini, and Mars Pathfinder missions at the Jet Propulsion Laboratory/California Institute of Technology in Pasadena, CA. She received a B.S. in mechanical engineering from Tulane University in New Orleans, LA, in 1981 and a master's degree and Ph.D. in aeronautics and astronautics from MIT in Cambridge, MA, in 1983 and 1987, respectively.



Robert E. Wallis is currently supervisor of the Microwave Systems Section of the RF Engineering Group at APL. He received his B.S. from the Pennsylvania State University in 1980 and his M.S. from Villanova University in 1983, both in electrical engineering. He joined the APL Space Department in 1999 and was the Lead Engineer for the MESSENGER Phased-Array System from 2000 to 2004. From 1983 to 1999, Mr. Wallis was with EMS Technologies, Inc. (formerly Electromagnetic Sciences Inc.), where he managed the Microwave Integrated Circuit (MIC) design group and led the development of switch matrices and SSPAs for spacecraft applications, including C-band SSPAs for the TOPEX mission, X-band SSPAs for the Mars98 and Stardust missions, and Ku-band SSPAs for the International Space Station. From 1980 to 1983, Mr. Wallis was with General Electric Space Systems Division in Valley Forge, Pennsylvania, as a member of the MIC design group.



M. Annette Mirantes is a member of the Senior Professional Staff at The Johns Hopkins University Applied Physics Laboratory. She received a B.S. in electrical engineering from Purdue University and an M.S. in systems software engineering from George Mason University. She previously developed flight software for numerous missions at Orbital Sciences Corporation, including the ORBCOMM constellation, the Far Ultraviolet Spectroscopic Explorer (FUSE), and the Solar Radiation and Climate Experiment (SORCE). At APL, she has been the main processor flight software lead for the MESSENGER program.



T. Adrian Hill is a member of the Senior Professional Staff in the Embedded Applications Group at The Johns Hopkins University Applied Physics Laboratory. He was the Flight Software Lead for the MESSENGER mission. Before joining the Laboratory in 2000, he developed embedded software at Raytheon, GTE Spacenet, and Westinghouse Corp. He has previously led flight software development for satellites, including the Submillimeter Wave Astronomy Satellite (SWAS) and the Hubble Space Telescope (HST). He has a B.S.E.E. from The State University of New York at Buffalo and a M.S.C.S. from The Johns Hopkins University.



Sheng Cheng is currently a senior microwave circuit design engineer in the Microwave Systems Section of the RF Engineering Group at The Johns Hopkins University Applied Physics Laboratory. He received his B.S. from the National Taiwan University in 1982 and his M.S. from The Johns Hopkins University in 1989, both in electrical engineering. He joined APL's Space Department in 1997.



Since then, he has been the lead engineer for the TIMED IEM Downlink Card and more recently the MESSENGER X-band SSPA. He has also been involved in the development of CONTOUR Uplink Down-Converter and the RF front end of the Digital Receiver IRAD project. From 1990 to 1997, Mr. Cheng was with the Whiting School of Engineering of The Johns Hopkins University. His work there involved the research and development of microwave circuit theory, design methodology, and measurement techniques. He also taught the microwave circuits classes in the Part-Time Engineering Program during that time and co-developed gEE-CAD, a microwave circuit CAD tool for instructional use. Prior to that, Mr. Cheng was with the LKC Technologies in Gaithersburg, Maryland, as an electronic circuit design engineer developing ophthalmologic electro-diagnostic equipment.

Jonathan R. Bruzzi is a member of the Associate Professional Staff in the RF Engineering Group at APL. He acted as lead engineer for the MESSENGER Low Gain Antennas and was responsible for the phased array control, calibration, and measurement test processes. He received his B.S.E. in electrical engineering in 1999 and his M.S.E. in electrical engineering in 2000, both from the University of Pennsylvania. He joined the APL Space Department in 2000, specializing in antennas, electromagnetics, and optical communications.



Karl Fielhauer is a senior engineer and supervisor in the RF Engineering Group of APL's Space Department. Mr. Fielhauer leads the Systems Engineering section within the APL's RF Engineering Group. He received a B.S. in 1985 from Lawrence Technological University in Southfield, Michigan, and an M.S.E.E. in 2002 from The Johns Hopkins University in Baltimore, Maryland. Before joining APL, Mr. Fielhauer worked for the Department of Defense and Litton's Amecom Division in College Park. Since joining APL's Space Department in 1997, he has focused primarily on the design and development of digital hardware for the TIMED and CONTOUR missions and their ground support equipment. Mr. Fielhauer was the Lead RF Communications Engineer on the CONTOUR Mission and has assumed the same role for the MESSENGER program. Mr. Fielhauer is a member of IEEE.

